Air Concentrations in Plunge Pools Due to Aerated Plunging High-Velocity Jets and Dynamic Pressures in Underlying Fissures

Rafael Duarte
PhD Candidate, Laboratory of Hydraulic Constructions (LCH), Ecole Polytechnique Fédérale de Lausanne (EPFL), Station 18, CH-1015 Lausanne, Switzerland. Email: rafael.duarte@epfl.ch

ABSTRACT: High-velocity plunging water jets, such as those formed by spillways of high-head dams, cause scour on the rock foundations. The scour process is the result of complex physical phenomena concerning the three media involved, namely, water, rock and air. Air is entrained in the jet during the travel through the air and at the impinging point into the plunge pool. The air bubbles flow in the plunge pool influence energy dissipation and dynamic pressures. The bubbles may also enter rock fissures, where they will completely change properties of the propagation of pressure waves. The detailed knowledge of air bubbles behavior in plunge pools and of their influence in pressure fluctuations in the water-rock interface and inside fissures under prototype conditions is still lacking. Froude, Weber and Reynolds dependent phenomenon, observations on near-prototype scale models and consideration of fully transient pressures are necessary to appropriately assess the effect of jet impingement and air entrainment in the development of rock scour. The objective of this study is to assess experimentally air concentrations at different positions throughout the shear layer of impinging aerated jets and relate them with the dynamic pressures occurring around a confined block located at the bottom of the plunge pool. The experimental facility can reproduce vertical near-prototype jets, whose velocities vary between 4.9 and 22.1 m/s, impinging in an 80 cm deep plunge pool. Corresponding pool depth - jet diameter ratio is 11.1, creating developed jet impact on the bottom. Compressed air is added to the jet by means of 6 small openings in the nozzle. Air-to-water ratios of the jets vary from 0 to 23%. A double fiber-optic probe is used in different depths and radial distances from the jet axis in the plunge pool. Thus, air concentration, bubble rate and the vertical component of flow velocity are obtained. A metallic cube, with a edge of 200 mm, is inserted into the bottom of the plunge pool representing a confined rock block, allowing to measure dynamic pressures at 12 points around it. Using a systematic experimental approach, for the first time dynamic pressures occurring around a confined block could be related to air concentrations in a plunge pool impacted by aerated near-prototype jets. Air concentrations, bubble rate and flow velocity at each position of a plunge pool impacted by aerated water jets are clearly influenced by two opposing features, namely, the kinetic energy reduction of the jet and the jet aeration itself. Furthermore, kinetic energy reduction governs the lowering of mean pressures and their oscillations on the water-rock interface and underlying fissures. These results are part of an on-going research that aims at a physically-based description of the influence of air entrainment for scour assessment.

KEY WORDS: Air entrainment, air-water interactions, hydraulic jets, rock scour, dynamic pressures.

1 INTRODUCTION

The entrainment of air by a plunging liquid jet into a pool is a subject of interest for researchers in many engineering problems. This phenomenon might be a desired feature in industrial applications, involving mixing and reacting of liquids and gases, or an issue to be avoided in other processes such as

the pouring of molton glass or metal, or when it causes degradation of the entraining fluid (McKeogh and Ervine, 1981).

In hydraulic engineering, the most common case is that of water jets issued from a flood release structure. Differently from the previous examples, these jets will present high velocities and turbulence when impacting the receiving plunge pool. At this point, the jet will be often composed by a compact core surrounded by a somehow developed and aerated outer layer. The jets carry a great amount of energy, and it is of major importance in hydraulics design to predict the erosion that they can produce on the bottom of the plunge pool.

The objective of the present paper is to assess air bubble dispersion features into a plunge pool impacted by high-velocity aerated jets and the corresponding dynamic pressures occurring at the water-rock interface and underlying fissures. For such, air concentration, bubble rate and flow velocity were measured in different points of the shear layer of the jet. Dynamic pressures were assessed around a block inserted into the bottom of the pool. Detailed results on dynamic pressures around a confined block as a function of jet aeration are presented in a companion paper (Duarte et al, 2013).

2 THEORETICAL ASPECTS

2.1 Brief description of rock scour process

Rock scour resulting from plunging water jets is a complex phenomenon, composed of a series of processes illustrated on Figure 1 (left). The design of the release structure will define jet geometry (hereby the diameter D_i for a circular jet or thickness B_i for a plane jet), velocity V_i and turbulence intensity T_u at issuance. These parameters, together with water properties such as density ρ_w, kinematic viscosity μ_w and the gravitational acceleration g will govern the jet during the trajectory through the air.

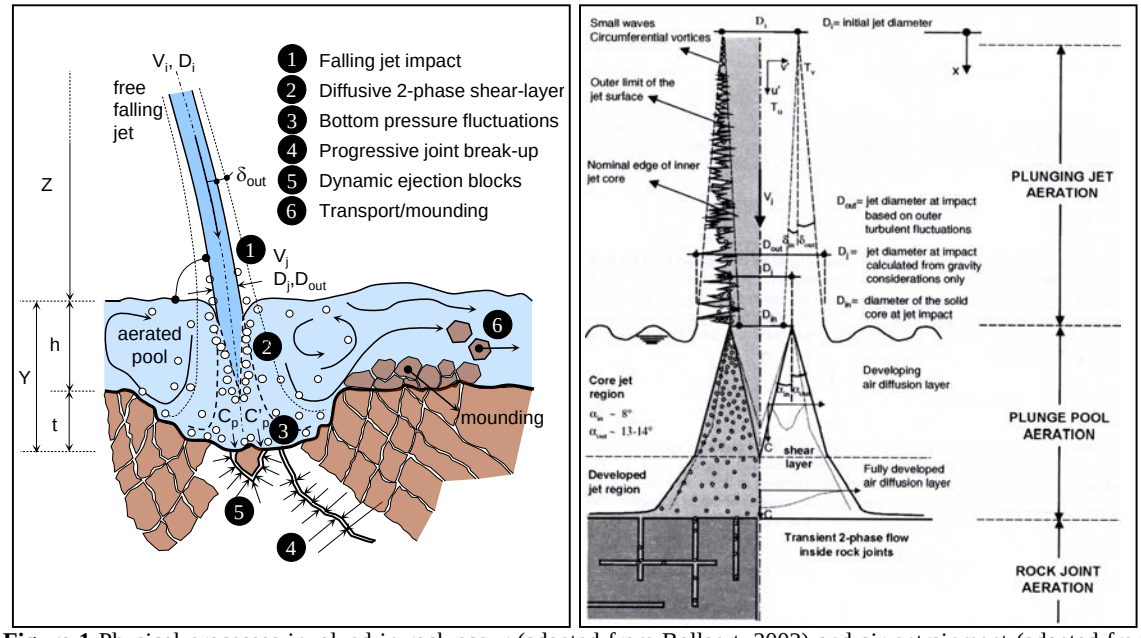

Figure 1 Physical processes involved in rock scour (adapted from Bollaert, 2002) and air entrainment (adapted from Ervine and Falvey, 1987)

The development of the free-falling water jet will be mainly a function of the turbulence intensity and the water surface tension σ_w (Ervine et al, 1997), and of the drop length Z. Surface tension will act in a way to keep the jet stable, while internal turbulence will create disturbances in the jet outer surface with increasing distance from the issuance point, establishing an increasing disturbed outer zone and a decreasing internal core (Figure 1, right).

The kinetic energy of the jet at impact E_k is the main parameter that governs scour development.

Diffusion in the plunge pool of depth Y will dissipate part of this energy. The remaining energy will load the rock bottom with dynamic pressures. These pressures will propagate inside rock joints as pressure waves. Bollaert and Schleiss (2005) showed that dynamic pressures inside closed-end rock joints can cause resonance and amplification effects. Furthermore, they highlighted the importance of considering the full fluctuation spectrum of the pressure signals instead of only the mean pressures for scour assessment.

Further joint break-up and fissure propagation occurs due to the dynamic pressures and as a function of rock characteristics. Finally, after a rock block is formed by completely connected fissures, it will be ejected from the rock as a function of the dynamic pressures and the resistance against the displacement. This process will continue until the process finds equilibrium at an ultimate pool depth Y_{eq}.

2.1 Air entrainment

Bin (1993) and Ervine (1998) provided complete air entrainment reviews that remain up to date. A plunging water jet transfers air into a receiving pool by two main aeration processes, namely jet air entrainment and plunge pool air entrainment (Figure 1, right). The first is related to the development of instabilities on the jet surface in the air. Air will occupy the empty spaces, and continuity dictates that the surrounding air will flow towards the jet. This can be seen by observing the mist formed around plunging high-velocity jets, which does not flow downwards in the same direction as the jet but slowly towards it (Ervine et al, 1997).

The second process is plunge pool air entrainment. For most practical applications in dam engineering high-velocity jets will impinge relatively undeveloped and air entrainment at the point of impact will be the most important source of aeration. Once inside the plunge pool, air bubbles will be submitted to buoyancy, as a function of its volume. Nevertheless, because air is a highly compressible fluid, buoyancy forces will tend to have little influence in high pressure zones. Air bubbles will be trapped inside the turbulent eddies of the water flow towards the bottom. The bubbles that reach the water-rock interface can enter rock fissures, form air pockets and change resonance properties of pressure waves flow (Bollaert, 2002).

The aeration provided by a water jet can be described by the air-to-water ratio β, defined by:

$$\beta = \frac{Q_a}{Q_w} \tag{1}$$

where Q_a is the air discharge and Q_w is the water discharge. The mean entrained air concentration C_a is defined by:

$$C_a = \frac{Q_a}{Q_w + Q_a} = \frac{\beta}{1+\beta} \tag{2}$$

Ervine and Falvey (1987) state that the mean pressures on the bottom of a plunge pool impacted by a jet will be reduced by jet aeration due to reduction of its kinetic energy. The kinetic energy per unit volume E_k is given by:

$$E_k = \rho_{aw} V_j^2 / 2 \tag{3}$$

where V_j is the jet velocity at the imping point and ρ_{aw} is the density of the air-water mixture. The dimension of the kinetic energy in Equation 3 [Pa] takes into consideration fluids of different mean densities. The density of the aerated jet ρ_{aw} is given by:

$$\rho_{aw} = \left(\frac{1}{1+\beta}\right)\rho_w + \left(\frac{\beta}{1+\beta}\right)\rho_a \tag{4}$$

in which ρ_w is the water density and ρ_a is the air density. Finally, the reduction of the kinetic energy of the jet caused by aeration can be obtained, which is equal to the mean entrained air concentration C_a.

$$1-\frac{E_{k(aeratedjet)}}{E_{k(nonaeratedjet)}}=\frac{Q_a}{Q_a+Q_w}=\frac{\beta}{1+\beta}=C_a \quad (5)$$

2 EXPERIMENTAL FACILITY

2.1 Physical model

A large experimental facility at the Laboratory of Hydraulic Constructions of the Ecole Polytechnique Fédérale de Lausanne allows reproducing near-prototype jet velocities up to 22.1 m/s, impinging on a 0.8 m deep plunge pool (Figure 2). On the bottom, a highly instrumented metallic 200 mm-sided cube inserted in a cavity represented a rock block embedded in an open 3D fissure of 1mm thickness. Dynamic pressures were measured at 12 positions along the transversal section of the cube; 4 on the water-rock interface, 4 in the vertical fissure and 4 in the horizontal fissure.

The jets were issued from a cylindrical nozzle with an internal diameter of 72 mm. The jets were actively aerated with compressed air through 6 small aluminium tubes uniformly distributed around the nozzle, 250 mm upstream of the issuance section.

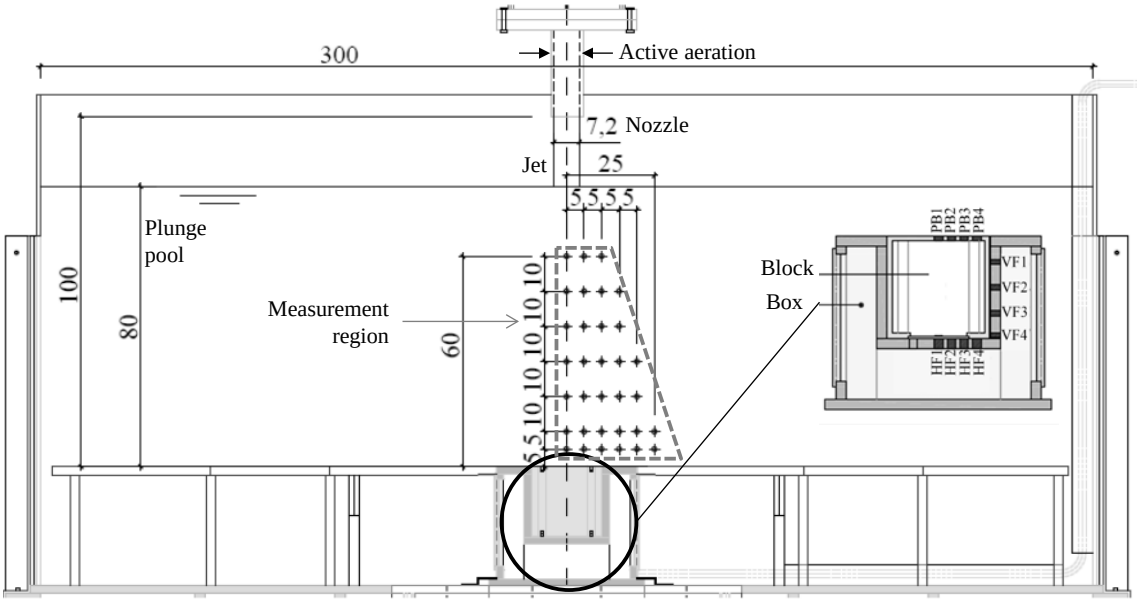

Figure 2 Experimental facility and positions for air and velocity measurements in the plunge pool (dimensions in cm). Detail of the cube and positions of the pressure transducers (adapted from Federspiel, 2011).

2.2 Instrumentation and data treatment

A double fiber-optic probe (Figure 3) was used to measure air concentration, the number of bubbles and bubble velocity in 33 different positions of the plunge pool (for measurement points in Figure 2). The system developed by RBI Instrumentation comprises 3 modules:

- The fiber-optic probe has a work principle based on the difference of refraction coefficients of water and air. Light pulses emitted through the probe are thus refracted from the sensitive cone-shaped tip surface when surrounded by water or reflected inwards when in presence of gas.
- An optoelectronic module emits the light signal to the tips and converts the reflected light signal into electric signal. The produced raw analog signal was set to 0V when the tip is in water and 5V when the tip is in gas. By a double threshold system, the module converted the analog signal into a digital Transistor-Transistor Logic (TTL) signal. The lower threshold was set to 1V and the upper threshold was 3V, resulting in a digital square signal.
- The third module is the acquisition card and the software ISO v2.09, responsible for acquisition and treatment routines.

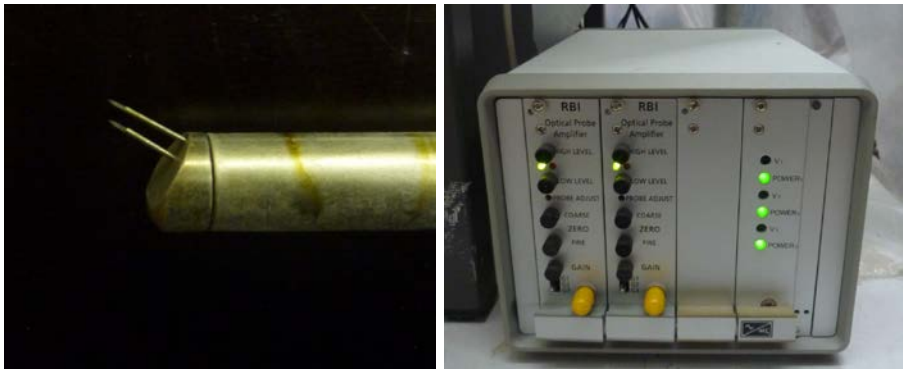

Figure 3 Detail of probe tips and optoelectronic module

By the treatment of the single probe signals air concentration and the number of bubbles can be obtained. The air concentration is defined as the relative amount of time that the probe tip is in gas, while the number of bubbles is obtained by counting the rising edges of the square signal. The component of bubble velocities in the direction of the tips alignment are obtained by the cross-correlation of the signals of the two probes, knowing that the distance between tips is 2.5 mm. It has to be noted that the obtained results are representative only for the vertical component of the velocity, direction chosen for the tips' alignment to enhance the analysis of velocity decay in the shear layer of the jet. Also, in the shear layer region, it is admitted that the bubbles' velocity is representative of the water flow velocity, as buoyancy effects will be negligible compared to the drag imposed by the turbulent flow.

Dynamic pressures around the instrumented block were obtained by 12 micro-pressure transducers of type KULITE HKM-375M-17-BAR-A. These sensors have a flush-mounted metal diaphragm with an absolute pressure range between 0 and 17 bars and a precision of ± 0.1% of the full scale output. The data acquisition device is a National Instruments (NI) card type USB-6259 series M. The NI device is driven with laboratory developed software running in the LabVIEW© environment.

2.3 Test program

The jets impinge in the center of the measurement block, fixed unable to move. The test program with the range of the tested parameters is given in Table 1.

Table 1 Overview of test program

Pool depth Y	Relative depth Y/D_i	Total discharge Q_{aw}	Mixture velocity V_{aw}	Jet aeration β
[m]	[-]	[l/s]	[m/s]	[%]
0.8	11.1 (developed jet)	20 to 90	4.9 to 22.1	0, 8, 15 and 23

For the fiber-optic probe measurements, three runs of 60s each were performed at each position shown in Figure 2. Air concentration, the number of bubbles and vertical velocities were obtained. The system is able to count up to 2.5 x 10^5 bubbles. Such limit has been reached for some test configurations, causing a stop in the acquisition before 60s. For this reason, results of bubbles rate are presented, defined as the obtained number of bubbles divided by the acquisition period, in bubbles/s.

The pressure transducers in the measurement box obtained 65'536 samples at an acquisition frequency of 1kHz. For assuring repeatability of the results, 3 runs were done for each configuration.

3 RESULTS AND DISCUSSION

3.1 Air concentration

The measured air concentration values in the shear layer region of the jets is represented graphically

in Figure 4, for a low-velocity jet (of V_{aw} = 7.4 m/s) and a high-velocity jet (of V_{aw} = 22.1 m/s), for the tested jet aerations. The graphs were plotted with the same color scale for comparison. It should be noted that the plotted region is 20 cm below the water surface and 5 cm above the bottom of the pool.

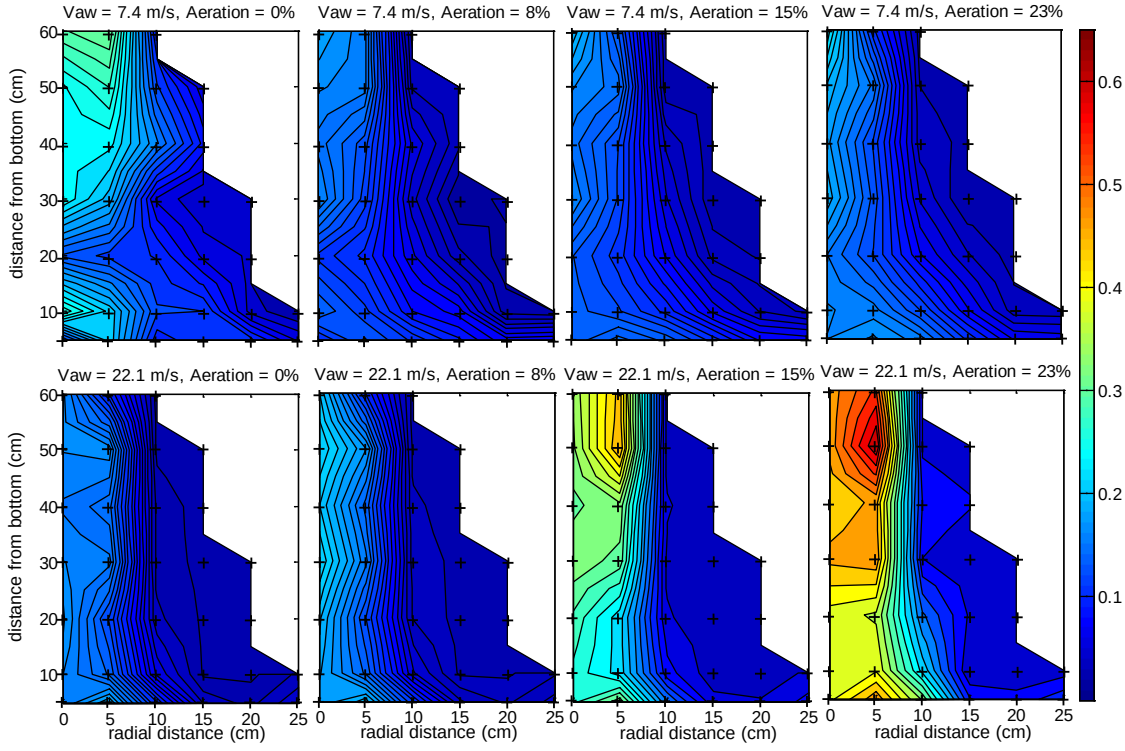

Figure 4 General view of air concentration results in the measurement region in the plunge pool. Above: V_{aw} = 7.4 m/s. Below: V_{aw} = 22.1m/s. Increasing jet aeration from left to right. Non-dimensional air concentration color scale [-].

For low-velocity jets (Figure 4, above), the reduction of the kinetic energy of the jet with increasing aeration can be noticed, as the bubbles penetrate less into the plunge pool. Visual observations confirmed this behavior. The non-aerated jet (left) has a more aerated region around the jet axis closer to the surface (between 30 and 60 cm from the bottom). It can be seen that this core progressively disappears with increasing jet aeration. The presence of the bottom has also an effect on air concentration values. This is reflected by the change in direction of the contour lines as the jet is diffused more and more close to the water-rock interface. For high-velocity jets (Figure 4, below) this is less pronounced.

The peaks of air concentration occur at the point 5 cm from jet axis close to the jet impact region. For high-velocity jets this was observed for the most aerated jets. This behavior indicates air entrainment at the plunge point. The jet has a radius of 3.6 cm and values of air concentration obtained above 60% can be explained by the proximity with the induction trumpet created by jet impact. This phenomenon was also observed by Brattberg and Chanson (1998), who developed relationships for air bubble dispersion in a plunge pool. Nevertheless, jet velocities tested in the present study are out of the range of these expressions.

In Figure 5 air concentration is shown as a function of jet velocity for two positions in the plunge pool, in the jet axis and 20 cm from jet axis, both 30 cm above the bottom. The graphs in Figure 5 confirm that two main features influence air concentrations in the plunge pool with opposed consequences. While the upstream jet aeration increases the amount of air in the plunge pool, the corresponding reduction of the jet's kinetic energy lowers air concentrations. The latter is predominant for lower velocities of the jet, where higher values of air concentration were obtained for the less aerated jets. On the other hand, for high-velocity jets, jet aeration overcomes the reduction of kinetic energy and air concentration grows following a linear trend.

Bubble rate as a function of the incoming jet velocity is shown in Figure 6 in the same positions

considered in Figure 5. The bubble rate does not take into account bubble size distribution and is a mere count of the bubbles divided per time of acquisition.

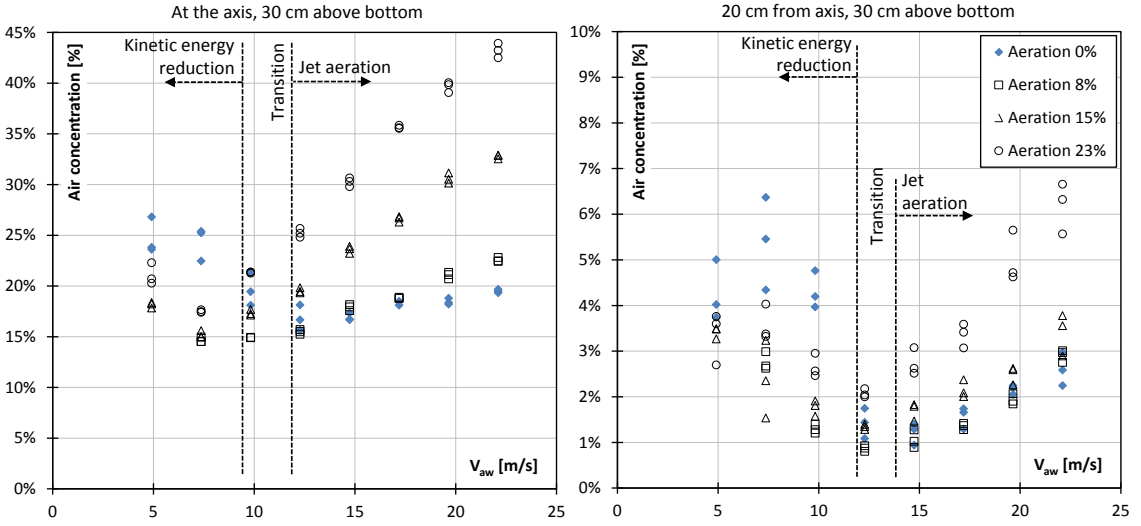

Figure 5 Air concentration as a function of jet velocity at the jet axis, 30cm above bottom (left) and 20cm from axis, 30cm above bottom (right)

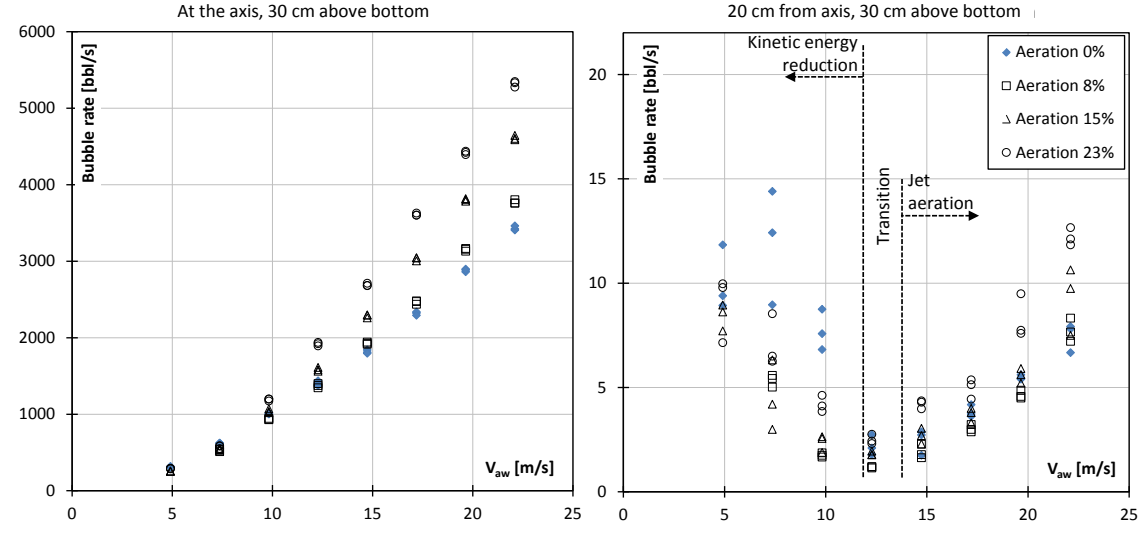

Figure 6 Bubble rate as a function of jet velocity at the jet axis, 30cm above bottom (left) and 20cm from axis, 30cm above bottom (right)

At the axis, the difference between regions influenced by kinetic energy reduction and jet aeration is barely noticeable in Figure 6, and the bubble rate has a clear parabolic trend with jet velocity. Far from the axis, again a region dominated by kinetic energy reduction at low-velocity jets can be seen. As it was the case for air concentrations, results inverse in a transition region, after which bubble rates as a function of jet velocities develop a parabolic trend.

3.2 Vertical velocity pattern in the dispersing jet region

Velocity measurements by cross-correlation of the signals from the two tips of the optic-fiber probe with a known offset gave good results. Nevertheless, data treatment has to be done carefully, especially

for high-velocity jets. Velocities above 10 m/s have seldom been measured with this technique (Manso, 2006).

The vertical components of flow velocity at each point are shown in Figure 7 for a jet velocity of 7.4 m/s and all tested jet aerations. Downward velocities are shown in colors from yellow to red, while upward values are highlighted in blue. The momentum shear layer is quite good visible by these vertical components. As in the case for air concentration discussed before, a direct effect of the kinetic energy reduction can be seen with the diminishing core of the downward velocity with increasing jet aeration.

In Figure 8 (left) flow velocities are shown as a function of the incoming jet velocity for the 2 extreme positions in the jet axis. Close to the bottom (5 cm), downward velocities increase with a parabolic trend for low-velocity jets. Close to the water surface (60 cm from the bottom) the quadratic tendency is inversed to a concave parabola that covers the whole range of tested jet velocities. It can be seen that velocity decay in the axis of the dissipating jet is maximum for low-velocity jets and lowers until it becomes almost inexistent for high-velocity jets.

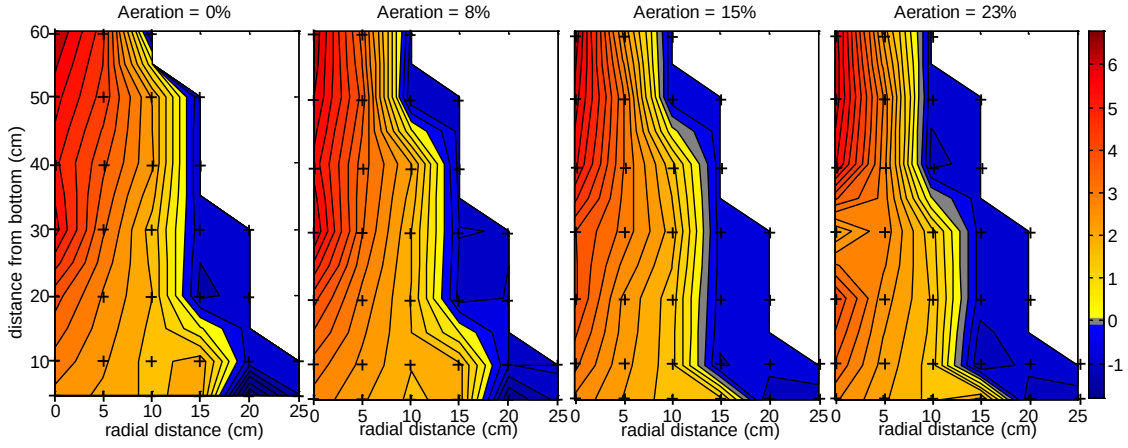

Figure 7 Vertical downward and upward velocity component for V_{aw} = 7.4 m/s. Velocity color scale in [m/s]

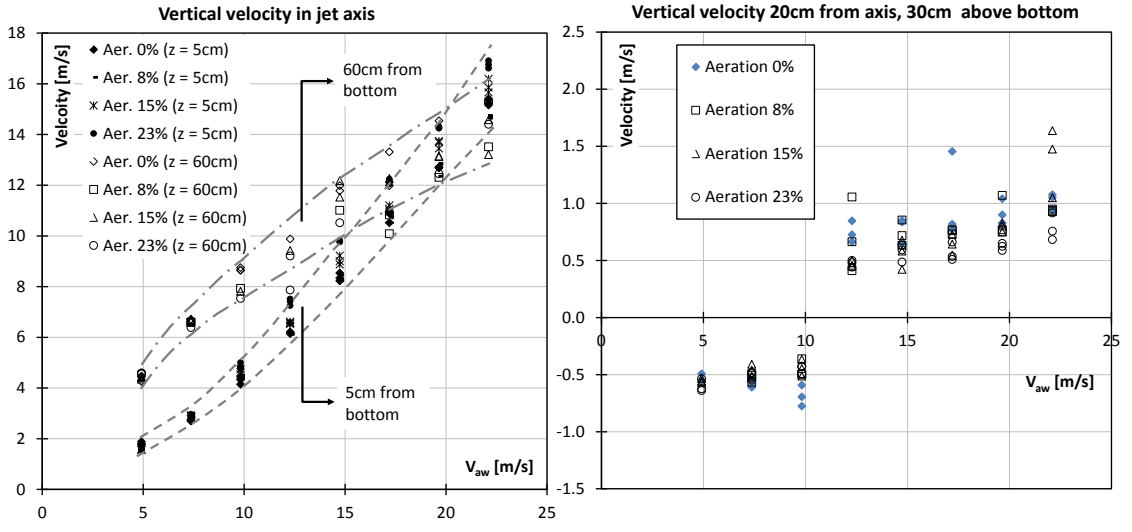

Figure 8 Vertical flow velocity as a function of incoming jet velocity. Left: In the axis for 2 different height (5 cm and 60 cm from bottom) and corresponding outer bounds. Right: 20 cm from axis, 30 cm above bottom

At a position 20cm from the jet axis (Figure 8, right), vertical velocities are obviously much smaller. Interesting to note is the change in signal of the flow as the incoming jet velocities increase, indicating the entrance in the shear layer of the jet.

3.3 Dynamic pressures in underlying fissures

The dynamic pressure data were analyzed with the mean pressures and RMS fluctuations. The corresponding non-dimensional coefficients C_p and C_p' are computed as:

$$C_p = \frac{(P_{mean} - P_{atm}) - \rho_w g Y}{\rho_{aw} V_j^2 / 2} \tag{5}$$

$$C_p^{'} = \frac{\sigma}{\rho_{aw} V_j^2 / 2} \tag{6}$$

where P_{mean} is the mean pressure [Pa], P_{atm} is the atmospheric pressure [Pa], g is the gravitational acceleration and σ is the RMS value of the pressure fluctuations [Pa].

The reductions of the coefficients C_p and C_p' were obtained for total jet velocities from 12.3m/s to 22.1m/s by dividing the coefficient by the corresponding value for the non-aerated jet. In Figure 9 the results and compared with the theoretical reduction according to Equation 5 (Ervine and Falvey, 1987). Lower jet velocities showed little effect on the pressures and are not shown.

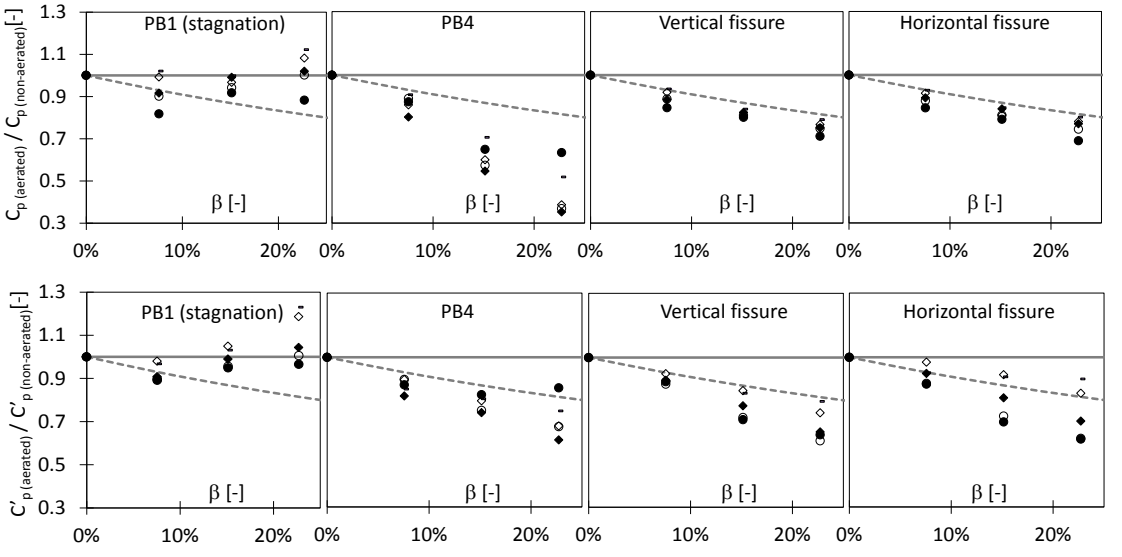

Figure 9 Reduction of mean pressures (above) and fluctuations (below) as a function of jet aeration for different positions around the block. (-): V_{aw} = 12.3m/s ; (◊): V_{aw} = 14.7m/s; (♦): V_{aw} = 17.2m/s; (○): V_{aw} = 19.6m/s; (●): V_{aw} = 22.1m/s. Dashed line: theoretical curve (Ervine and Falvey, 1987). See Figure 2 for transducers' positions.

According to Figure 9, except for stagnation, mean pressure reduction increases clearly with jet aeration. The reductions of mean pressures in the vertical and horizontal fissures are very similar and approach the theoretical curve. At the top of the block at PB4 the reductions are even more pronounced. Nevertheless, at stagnation mean pressures are not reduced with increasing aeration.

This is also the case for pressure fluctuations. At stagnation, values even seem to slowly increase, especially for the lower velocity jets, which would present a more developed feature at the bottom of the pool. Pressure fluctuations reduce in the other positions approaching the reduction of the kinetic energy. It is interesting to note that the horizontal fissure presents a slightly lower reduction of the fluctuations than the vertical fissures.

4 CONCLUSIONS

The influence of the aeration of impinging water jets on air bubbles dispersion patterns in the plunge pool and on dynamic pressures on the water-rock interface and underlying fissures was studied experimentally. With a double fiber-optic probe, air concentration, bubble rate and the vertical component of flow velocity were measured in 33 positions of the impacting jet shear layer. The corresponding

dynamic pressures were measured at 12 positions around a block placed on the bottom, being 4 on the water-rock interface, 4 in the vertical fissure and 4 in the horizontal fissure.

Aeration of the jet and the resulting kinetic energy reduction have opposed effects on air bubble dispersion parameters in the plunge pool. While jet aeration increases air concentrations in the pool, the corresponding energy reduction decreases the bubbles penetration and, consequently, air concentration. Kinetic energy reduction is predominant for low-velocity jets, while the incoming jet aeration is more relevant for high-velocity jets.

Aerated high-velocity jets produce lower mean pressures and oscillations, both on the water-rock interface and inside fissures, which is governed by the resulting kinetic energy reduction. This was observed for all positions around the block, except for stagnation where the results are still inconclusive.

This paper presents a first analysis of experiments undertaken in the frame of a broader research on the influence of jet aeration on rock scour that has the objective of developing a complete physically-based description of the governing processes and parameters. In this context, the present paper analyses and describes these results, focusing on the main physical phenomena, without proposition of empirical formulations. Future steps include: a) the use of submerged jets, which will allow the analysis of jet aeration as representative of the total entrained air and enable conclusions on plunge point air entrainment of the plunging jets presented in this paper; b) the assessment of jet issuance characteristics such as turbulence intensity and velocity distribution in the transversal section; and c) different block configurations, including a jet impinging directly on the fissures and the block free to move, for a complete description of block ejection.

ACKNOWLEDGEMENT

The research project is funded by the Fundação para a Ciência e a Tecnologia (FCT, Portugal, Grant No. SFPH/BD/51074/2010) and supervised by Prof. Anton Schleiss, from the Ecole Polytechnique Fédérale de Lausanne, and Prof. António Pinheiro, from the Instituto Superior Técnico, Technical University of Lisbon.

References

Bin, A. K., 1993. Gas entrainment by plunging liquid jets. Chem. Eng. Sci. 48:3585–630

Bollaert, E.F.R., 2002. Influence of transient water pressures in joints on the formation of rock scour due to high-velocity jet impact, PhD Dissertation, EPFL, March 2002, Lausanne, Switzerland.

Bollaert E.F.R.; Schleiss A.J. (2005): Physically based model for evaluation of rock scour due to high-velocity jet impact, Journal of Hydraulic Engineering, 131(3), 153-165.

Brattberg, T.; Chanson, H. (1998). Air entrapment and air bubble dispersion at two-dimensional plunging water jets, Chemical Engineering Science 53(24): 4113-4127.

Duarte, R., Schleiss, A., Pinheiro, A., (2013). Dynamic Pressure Distribution around a Fixed Confined Block Impacted by Plunging and Aerated Water Jets, Proceedings of the 35th IAHR World Congress, 8-13 Sept. 2013, Chengdu, China

Ervine, D.A.; Falvey, H.T., 1987. Behavior of Turbulent Water Jets in the Atmosphere and in Plunge Pools, Proceedings of the Institution of Civil Engineers, Part 2, pp. 295-314.

Ervine, D.A., 1998. Air Entrainment in Hydraulic Structures: a Review, Proceedings of the Institution of Civil Engineers, Water, Marit. And Energy, Vol. 130, pp. 142-153.

Ervine, D.A.; Falvey, H.T.; Withers, W., 1997. Pressure Fluctuations on Plunge Pool Floors, Journal of Hydraulic Research, Vol. 35, N° 2, pp. 257-279.

Federspiel, M.P.E.A. (2011): Response of an embedded block impacted by high-velocity jets. Communication 47, Laboratory of Hydraulic Constructions, Ed. A. Schleiss, LCH-EPFL, Lausanne, ISSN 1661-1179.

Manso, P. (2006). The influence of pool geometry and induced flow patterns in rock scour by high-velocity plunging jets, Communication 25, Laboratory of Hydraulic Constructions, Ed. A. Schleiss, LCH-EPFL, Lausanne, ISSN 1661-1179.

McKeogh EJ, Ervine DA., 1981. Air entrainment rate and diffusion pattern of plunging liquid jets. Chem. Eng. Sci. 36:1161–72